Published in final edited form as:

Oncogene. 2010 November 18; 29(46): 6115–6124. doi:10.1038/onc.2010.350.

Tenascin-C promotes melanoma progression by maintaining the ABCB5-positive side population

Mizuho Fukunaga-Kalabis[1], **Gabriela Martinez**[1], **Thierry-Thien K. Nguyen**[1], **Diana Kim**[1], **Ademi Santiago-Walker**[1], **Alexander Roesch**[1], and **Meenhard Herlyn**[1]

[1]Molecular and Cellular Oncogenesis Program, The Wistar Institute, Philadelphia, PA, 19104

Abstract

Tenascin-C (TNC) is highly expressed in melanoma; however, little is known about its functions. Recent studies indicate that TNC plays a role within the stem cell niche. We hypothesized that TNC creates a specific environment for melanoma cells to exhibit a stem cell-like phenotype, driving tumor growth and evading conventional therapies. TNC expression was strongly up-regulated in melanoma cells grown as 3D spheres (enriched for stem-like cells) when compared to adherent cells. Down-modulation of TNC by shRNA-lentiviruses significantly decreased the growth of melanoma spheres. The incidence of pulmonary metastases after intravenous injection of TNC knockdown cells was significantly lower in NOD/SCID IL2Rγ^{null} mice compared to control cells. Melanoma spheres contain and increased number of side population (SP) cells, which exhibited stem cell characteristics and the potential for drug resistance due to their high efflux capacity. Knockdown of TNC dramatically decreased the SP fraction in melanoma spheres and lowered their resistance to doxorubicin treatment, likely due to the down-regulation of multiple ABC transporters, including ABCB5. These data suggest that TNC plays a critical role in melanoma progression by mediating protective signals in the therapy-resistant population of melanoma.

Introduction

Tenascin-C (TNC) is a secreted extracellular matrix glycoprotein and a member of the matricellular protein family. Matricellular proteins are non-structural components of the ECM which regulate cell-matrix interactions and promote signaling via communication with integrins, extracellular matrix components, growth factors, and cytokines (Bornstein & Sage, 2002). Matricellular proteins function in diverse biological processes including cell adhesion, proliferation, migration, differentiation, and survival with effects being dependent on cell type and tissue context (Brigstock, 1999; Perbal, 2004). TNC is a large, 220-320 kDa protein containing a N-terminal oligomerization motif of EGF-like, fibronectin type III, and fibrinogen-like domains (Orend & Chiquet-Ehrismann, 2006). TNC is highly expressed

Correspondence to Meenhard Herlyn, The Wistar Institute, 3601 Spruce Street, Philadelphia, PA, 19104, USA. Phone: +1(215) 898-3950, Fax: +1(215) 898-0980, herlynm@wistar.org.

Conflict of Interest

The authors declare no conflict of interest.

during organogenesis. Though absent or expressed at low levels in adult tissues, TNC can be induced during tissue remodeling, inflammation, and tumorigenesis (Chiquet-Ehrismann & Chiquet, 2003). In normal human skin, TNC levels are low; however, increased expression of TNC is observed in melanoma. The majority of human melanoma cell lines express and secrete TNC (Herlyn *et al.*, 1991). TNC expression is known to correlate with melanoma progression and metastasis (Tuominen & Kallioinen, 1994). However, it remains to be determined if TNC is functionally involved in melanoma pathogenesis.

Accumulating evidence supports the existence of stem cell-like populations in human tumors which initiate and sustain tumor growth (Reya *et al.*, 2001; Wicha *et al.*, 2006). Initially, it was thought that only a small fraction of cells within a tumor could seed a new tumor in an immunocompromised host; however, a recent study demonstrated that stem cell-like populations with tumorigenic potential are likely common in melanoma (Quintana *et al.*, 2008). Indeed, we have recently shown that the acquisition of stem cell-like characteristics is a dynamic process in melanoma (Roesch *et al.* 2010). It is likely that microenvironmental cues contribute to the development of stemness. Matricellular proteins are known to play a role in the maintenance and quiescence of the stem cell niche (Nilsson *et al.*, 2005). Murine Tnc can regulate neuronal stem cell fate by modulating sensitivity to growth factors (Garcion *et al.*, 2004). TNC expression is also up-regulated in the bulge region of the human hair follicle, where it may contribute to the hair follicle stem cell niche (Kloepper *et al.*, 2008). The elevated levels of TNC in advanced melanomas and stem cell niches prompted us to examine whether this molecule contributes to melanoma progression.

Results

TNC is highly expressed in melanomas and its expression is increased in stem cell-like subpopulations

To investigate the potential involvement of TNC in melanoma development and progression, we quantitatively examined TNC expression in melanoma cell lines representing different stages of tumor progression. While TNC was absent in human epidermal melanocytes, it was highly expressed in most of the advanced melanoma cell lines grown in monolayer. The weakly tumorigenic radial growth phase (RGP) melanoma cell line WM35 and the moderately tumorigenic cell line WM164 were the two exceptions, expressing very little TNC (Figure 1A).

Strong TNC expression has been reported in neuronal and skin stem cell niches (Garcion *et al.*, 2004; Kloepper *et al.*, 2008). Recently, we reported that sphere-forming melanoma cells, termed “melanoma spheres”, exhibit stem cell-like characteristics when cultured in human embryonic stem cell medium (Fang *et al.*, 2005). Interestingly, TNC expression was up-regulated in three out of four melanoma sphere lines grown in stem cell medium, compared to their adherent counterpart lines grown in conventional melanoma growth medium (Figure 1B). Notably WM35 sphere cells exhibited a robust induction of TNC expression. WM115 sphere line was the only cell line which did not show up-regulation of TNC expression compared to WM115 adherent cells. To test whether factors involved in the stem cell medium up-regulate TNC expression, we incubated adherent cell lines WM35 and WM3734 with hESCM4 for up to 72 hours. During this incubation time, sphere formation was not

induced in the lines. The transient up-regulation of TNC expression was observed in both adherent lines (peaked at 24 h for WM35, 48h for WM3734, and then decreased by the 72h time point) (Supplementary Figure 1). The data suggest that hESCM4-derived factors can up-regulate TNC expression in adherent melanoma lines; however 3D sphere formation is required for sustained TNC expression. The increase in TNC expression in melanoma spheres led us to hypothesize that TNC may contribute to the generation of a microenvironment conducive to stem cell-like growth.

TNC supports the growth of melanoma spheres *in vitro*

TNC promotes overall survival of neuronal cells after cell detachment (Jones *et al.*, 1997) by preventing anoikis (Marchionini *et al.*, 2003). We determined whether TNC regulates the growth of melanoma spheres. WM3734 cells, infected with lentivirus encoding shRNAs to TNC (sh_TNC_A and sh_TNC_C), showed an 80-90% decrease in TNC protein expression when compared to control vector-infected cells (sh_Cont) (Figure 2A). Attenuation of TNC did not affect the growth of WM3734 adherent cells over a three-day time course (Figure 2B, left panel). In contrast, sh_TNC induced a significant decrease in the growth of WM3734 spheres (Figure 2B, right panel). This observation suggests that TNC maintains cell survival and growth of melanoma sphere cells.

TNC knockdown decreases *in vivo* lung colonization

To investigate whether TNC promotes progression of melanomas *in vivo*, we tested lung colony formation in an experimental metastasis model by injecting 2×10^5 WM3734 sh_Cont and WM3734 sh_TNC cells intravenously into nonobese diabetic/severe combined immunodeficient interleukin 2 receptor γ chain null (NOD/SCID IL2Rγ^{null} or NGS) mice. After 8 weeks, the mice were sacrificed and lung samples were collected for analyses of metastases. Significantly fewer colonies developed in the lungs of mice injected with WM3734 sh_TNC_A and sh_TNC_C cells, compared to the WM3734 sh_Cont cell–injected group (Figures 3A and 3B). The lungs injected with control cells demonstrated destruction of lung parenchyma with alveolar collapse caused by tumor obstruction, edema, and hemorrhage, while the large part of the lungs injected with sh_TNC cells are composed of intact alveoli. Figure 3C shows the percentage of tumor size per total lung area. In contrast, there was no difference in tumor growth when WM3734 sh_Cont cells and WM3734 sh_TNC cells were subcutaneously injected into NOD/SCID IL2Rγ^{null} mice (Figure 3D). These data suggest that decreased lung colonization in TNC knockdown cells is not due to the disturbance of anchorage-dependent growth, but rather due to the decreased survival of injected non-adherent cells.

Melanoma spheres contain a side population expressing ABCB5

Sphere-forming melanoma cells are multipotent, similar to neural crest stem cells (Fang *et al.*, 2005). To examine whether these cells share other characteristics with somatic stem cells, such as high chemical efflux capacity, we performed the Hoechst dye exclusion assay on sphere forming melanoma cell lines WM35, WM3734, and WM115. Differences in intensity of Hoechst dye signal usually indicate cell cycle because it binds to DNA. However, when Hoechst dye fluorescence detected by UV laser is displayed simultaneously

by red and blue emission wavelengths, it is observed that a gradient of Hoechst dye intensity is seen as a comma-like region on the bottom-left portion of the X-Y plot. The tip of the comma-like region forms a dim tail extending from the normal G1 cell population. A subpopulation of these cells, termed as “side population” (SP) and exhibits high efflux capacity for antimitotic drugs or the dye Hoechst 33342, has been identified in several tissues of mammalian species (Goodell *et al.*, 1996). The heightened efflux capacity of the SP is mediated primarily through the expression of the ATP-binding cassette (ABC) transporters. Consistent with a previous report showing that SP cells are present in human melanoma cell lines (Grichnik *et al.*, 2006), both WM35 and WM3734 melanoma cell lines contained SP cells ranging from 2% to 8% of total cells (Figure 4A). Interestingly, clear SP was not observed in WM115 line which lacked TNC induction in sphere cultures. The SP profile was more prominent in melanoma spheres than in their adherent counterparts (Figure 4B), indicating an increase of ABC transporter function in sphere-forming cells. ABCG2 (BCRP1) is a major pump mediating the SP phenotype (Scharenberg *et al.*, 2002). To examine whether ABCG2 expression correlated with our SP, melanoma spheres were stained with Hoechst 33342 for subsequent sorting of SP and major population (MP) cells (Supplementary Figure 2). Quantitative real-time PCR was then performed on both populations. Contrary to our expectations, the expression of *ABCG2* was decreased in the SP of WM3734 cells when compared to that of the MP (Figure 4C). Similar results were obtained for WM35 melanoma sphere cells (data not shown). ABCB1 (MDR1), another ABC transporter, also regulates the SP phenotype (Jonker *et al.*, 2005; Mouthon *et al.*, 2006); however, its expression was not detectable in WM3734 cells. Neither *ABCG2* nor *ABCB1* were expressed in WM35 cells (data not shown). ABCB5, a novel transporter similar to ABCB1, mediates doxorubicin drug resistance in melanoma (Frank et al., 2005). Pretreatment with verapamil resulted in a shift of the dose response curves of doxorubicin, suggesting verapamil blocks ABCB5 from ejecting doxorubicin (Supplementary Figure 3). SP cells in both the WM3734 and WM35 cell lines expressed higher levels of *ABCB5* than the MP cells (Figure 4D), indicating that ABCB5 participates in the maintenance of the SP phenotype. Furthermore, WM3734 sphere cells show higher expression levels of ABCB5 compared to WM115 sphere cells (Figure 4E). To determine whether SP cells are resistant to anticancer drugs that are ABCB5 substrates, we tested the sensitivity of WM3734 SP and MP cells to doxorubicin. After exposure to doxorubicin, the net growth of SP cells was notably higher than that of non-SP cells (Figure 4F).

TNC knockdown decreases the side population in melanoma spheres

Because it is known that melanoma spheres contain a significant number of cells with stem cell-like properties such as multipotency and high efflux capacity, and that TNC supports the growth of spheres, we next evaluated whether TNC modulates the SP phenotype in melanoma. The down-modulation of TNC induced a significant decrease in the SP fraction of both WM3734 and WM35 melanoma spheres (Figure 5A). Next, we analyzed by quantitative real-time PCR whether TNC regulates the expression of ABC transporters. The expression of *ABCB5* was down-regulated in cells stably transduced with sh_TNC vectors versus those transduced with a control vector (Figure 5B). Protein analysis also supported this observation (Figure 5C). Incubation with 10 μg/ml human TNC for 24 hours up-regulated the expression of *ABCB5* in both WM115 melanoma spheres and WM3734

adherent cells (Figure 5D). In addition, culturing the same cell lines in the presence of another extracellular matrix gelatin did not induce significant up-regulation compared to non-treated control cells. These data strongly suggest that TNC plays a role in maintaining the SP phenotype by either regulating the expression of ABCB5 or supporting the growth of the ABCB5 positive cell population. Among other tested ABC transporters the sh_TNC cells exhibited a minor decrease in *ABCB4* (*MDR3*), another gene that confers multidrug resistance. The cholesterol pump ABCA1 was also down-regulated in sh_TNC cells. Taken together, these studies indicate that TNC regulates the expression of multiple ABC transporters.

TNC knockdown sensitizes melanoma cells to doxorubicin

Our observation that the reduction of TNC decreases the SP fraction expressing ABCB5 in melanoma spheres, indicated that TNC likely confers resistance to doxorubicin. We tested whether down-modulation of TNC sensitizes melanoma cells to doxorubicin. To minimize the impact of factors in the culture medium, doxorubicin resistance was tested in medium which had been conditioned for 7 days on each respective cell line. Indeed, knockdown of TNC sensitized WM3734 and WM35 cells to doxorubicin, resulting in a significant shift of the dose response curve (Figure 6A). The percentage of apoptotic cells was then assessed by propidium iodide staining. Compared to WM3734 sh_Cont cells, which were resistant when treated with 2 μM of doxorubicin for 24 hours, WM3734 sh_TNC cells showed a significantly increased rate of apoptosis (Figure 6B).

Doxorubicin is a substrate of ABC transporters such as ABCB1, ABCB5, ABCG1, and ABCG2. Because ABCB1 and ABCG1 were only weakly expressed by the WM3734 cell line (data not shown) and the doxorubicin-resistant SP fraction was not enriched for ABCG2 (Figure 4C), it is likely that the decrease in doxorubicin resistance in TNC knockdown cells is due to the down-regulation of ABCB5. In contrast, doxorubicin resistance was markedly increased in WM115 melanoma spheres treated with 10 μg/ml TNC (Figure 6C). Presence of gelatin did not modify the resistance.

Discussion

The expression of specific ECM proteins, including TNC, is associated with drug resistance and disease progression of malignant neoplasms (Helleman *et al.*, 2008; Sethi *et al.*, 1999; Villuendas *et al.*, 2006); however, the exact mechanisms of how TNC contributes to tumor development remain unclear. Here, we demonstrate that TNC plays a role in mediating cell growth and survival of drug resistant melanoma SP cells. SP cells in some solid tumors have higher metastatic abilities than non-SP cells (Kabashima *et al.*, 2009; Nishii *et al.*, 2009). In agreement with this, the incidence of pulmonary metastasis after tail vein injection was significantly lower in NSG mice injected with TNC knockdown melanoma cells than in mice injected with control cells.

Major microenvironmental changes underlying metastasis include the clustered migration of cancer cells, ECM degradation, paracrine loops of released growth factors, and/or the induction of adhesion ligands in stromal cells (Bidard *et al.*, 2007). For most cells, TNC acts as an anti-adhesive molecule. When presented as a soluble protein to cells in a strong

adhesive state, TNC induces a rapid transition of cells to an intermediate state of adhesiveness (Murphy-Ullrich, 2001). Our data demonstrate that the down-modulation of TNC dramatically reduced the growth of 3D melanoma spheres, suggesting that the regulation of adhesion by TNC contributes to cancer progression by preventing cell death from anoikis. Furthermore, TNC-depleted melanoma cells lost their SP phenotype and became sensitized to doxorubicin treatment, indicating that a survival mechanism of melanoma cells during chemotherapy may be to embed in a matrix rich in matricellular proteins.

Increasing evidence indicates that the growth of many solid tumors is driven by a subset of cancer cells, tumor-initiating cells, capable of initiating and driving tumor growth (Dick, 2008); however, it remains unclear whether melanoma follows a hierarchical cancer stem cell model. Frank and co-workers reported that only ABCB5-positive melanoma cells showed tumor-initiating capacities in NOD/SCID mice (Schatton *et al.*, 2008). Conversely, the Morrison group showed that the majority of melanoma cells can initiate tumors in the more immunocompromised NSG (NOD/SCID IL2Rγ^{null}) mice when co-injected with Matrigel, regardless of the expression of specific markers, such as CD166 or CD133, which correlate with the expression of ABCB5 (Quintana *et al.*, 2008). Although it is not clear which of the models is more representative of human melanomas (Refaeli *et al.*, 2009), the Frank group's data point to the importance of the ABCB5 melanoma cell population for tumor initiation under more restricted conditions. Previous studies have revealed that the ABC transporter family proteins play biological roles besides drug resistance. For example, ABCB1 is functionally related to proliferation of colon cancer cells (Katoh *et al.*, 2008); ABCG2 has a role in ES cells pumping out protoporphyrin to maintain self-renewal capacity (Susanto *et al.*, 2008). Our data demonstrate that the disruption of TNC decreases the expression of ABCB5 in melanoma spheres and leads to a dramatic reduction of *in vivo* lung colonization. Taken together, there is accumulating evidence that ABCB5 is a critical a participant in melanoma tumor initiation.

The molecular pathways underlying the regulation of the expression of ABC transporters are not clear. However, accumulating data suggest that the phosphoinositol-3 kinase (PI3K) pathway is involved. Increased expression of ABCB1 in hepatoma cells is mediated by multiple effectors of PI3K signaling, including AKT and Rac1 (Kuo *et al.*, 2002). The PI3K inhibitor LY294002 decreased the expression of ABCG2 in leukemia cells (Nakanishi *et al.*, 2006). Inhibition of AKT or PI3K also regulated ABCA3 (Matsuzaki *et al.*, 2008) in alveolar Type II cells. Interestingly, TNC is known to activate AKT to prevent apoptosis in serum-starved chondrosarcoma cells (Jang & Chung, 2005). Recently, both TNC and PI3K were, independently, found to be necessary for PDGFR expression (Cohen *et al.*, 2009; Zhang *et al.*, 2007). These studies strongly suggest that the TNC-mediated biological phenotype is dependent on the PI3K signaling pathway. Consistent with this hypothesis, LY294002 reduced the SP phenotype in melanoma cells (data not shown).

In conclusion, we have shown here that TNC plays a critical role in melanoma progression by providing a unique microenvironment supporting a therapy-resistant population of melanoma cells capable of surviving during metastasis and seeding in the lungs. Further studies elucidating the mechanisms that underlie the evolution of the drug resistant SP

phenotype during melanoma progression may lead to the development of novel strategies against this deadly disease.

Materials and methods

Cell culture

Human melanoma cell lines (WM35, WM115, WM793, WM164, WM278, 1205Lu, 451Lu, WM3248 and WM3734) were isolated as previously described (Fang *et al.*, 2005). Two types of media were used for growing melanoma cells: (a) mouse embryonic fibroblast (MEF)–conditioned human embryonic stem cell (hESC) medium (Thomson *et al.*, 1998; Xu *et al.*, 2001). Before use, MEF conditioned medium was mixed with fresh hESC medium at a ratio of 3:1 and supplemented with basic fibroblast growth factor (bFGF) at 4 ng/mL. We termed this medium “hESCM4”. (b) Mel 2% melanoma growth medium, which was used to establish conventional adherent melanoma cell lines. It consisted of MCDB 153 medium (Sigma, St. Louis, MO; 4 parts), L15 medium (Invitrogen; 1 part), 2% fetal bovine serum (FBS), 5 μg/mL insulin (Sigma), and 1.68 mM calcium chloride. Normal human primary melanocytes and fibroblasts were isolated from the human epidermis of neonatal foreskins and cultured as described (Fukunaga-Kalabis *et al.*, 2006; Hsu *et al.*, 1998). 293T cells were cultured in DMEM (Invitrogen, Carlsbad, CA) supplemented with 10% FBS.

Viral vectors for knockdown

The mammalian expression vector, H1UG-1, derived from the FG12 lentiviral vector (Qin *et al.*, 2003), was used to produce lentiviral RNAi vectors. DNA sequences encoding shRNA targeting *TNC* were cloned into *Bam*H1 and *Xho*I sites under the control of the HuH1 promoter. The original DNA sequences encoding for the shRNAs targeting *TNC* mRNA were as follows: sh_TNC_A: 5′-gaagagcattcctgtcagc-3′ and sh_TNC_C: 5′-gttgacaaccttctggtt-3′. The DNA sequence encoding for the control non-targeting shRNA was 5′-gctgcaaaggacagtgcacctttc-3′. The lentivirus was produced by co-transfection of human embryonic kidney 293T cells with four plasmids: a packaging defective helper construct, a Rev plasmid, a plasmid coding for a heterologous envelope protein, and the H1UG-1 vector construct harboring the selected shRNA sequence.

Hoechst 33342 Staining and Flow Cytometry

Cells were dissociated into a single cell-suspension and resuspended at 10^6 cells/ml in Hank’s balanced salt solution containing 2% FBS and10 mM HEPES. Cells were preincubated at 37 °C for 30 min with or without 50 μM verapamil (Sigma-Aldrich, St. Louis, MO) to inhibit the ABC transporters, and then incubated for 120 min at 37 °C with 5 μg/ml Hoechst 33342 (Sigma-Aldrich). Cells were cooled on ice for 10 min, washed, and then incubated in ice-cold HBSS supplemented with 2% FCS, 10 mM HEPES, and 2 μg/mL propidium iodide (Sigma-Aldrich) at 4°C for 10 min to determine proportion of dead cells. The cells were then analyzed in a LSR II fluorescence-activated cell sorter (BD Biosciences, San Jose, CA) or sorted on a FACSDiva (BD Biosciences) by using blue laser (488 nm) to detect propidium iodide and using UV laser (355 nm) to detect Hoechst-DNA binding. A 610-nm short-pass dichroic mirror with 670 LP and 450 BP 20 detection filters for red and

blue emission wavelengths, respectively, were used. The data were analyzed by FlowJo (Tree Star, Inc. Ashland, OR).

MTS assay

For the measurement of net growth, cells were seeded at a density of 1000 cells per well in 96-well plates. Cell growth was monitored for the following 96 hours by MTS assay (Promega Corp., Madison, WI). To determine *in vitro* drug cytotoxicity, cells were dissociated into a single cell-suspension in hESCM4 medium and plated in 96-well plates at a concentration of 10,000 cells/well. After 24 hours, various concentrations of doxorubicin were added. The MTS assay was performed 72 hours post drug treatment according to the manufacturer's protocol (Promega Corp., Madison, WI). For sh_TNC lines, cells were dissociated into a single cell-suspension in hESCM4 medium that had been conditioned for 7 days with each lentiviral infected cell line, and were then plated in 96-well plates at a concentration of 10,000 cells/well. After 24 hours, various concentrations of doxorubicin were added. The MTS assay was performed 72 hours later. To test the effect of exogenous TNC, WM115 sphere cells were dissociated into single cell-suspensions in hES medium and plated in 96-well plates at a concentration of 10,000 cells/well with or without 10 μg/ml of human purified TNC (Millipore Corp., Billerica, MA). Twenty-four hours later, various concentrations of doxorubicin were added. The MTS assays were performed 72 hours post drug treatment. The net growth inhibition was defined as follows: [the OD value of cells within chemotherapeutic drug-treated wells/the OD value of cells within –untreated wells].

Quantitative real-time PCR

mRNA was isolated from cells immediately after sorting by using the RNeasy kit (Qiagen) and reverse transcribed into cDNA with SuperScript III (Invitrogen) as per the manufacturer's instructions. Gene-specific primers for SYBR Green real-time PCR were designed as follows: ABCB5, 5′-TCTGGCCCCTCAAACCTCACC-3′ (forward), 5′-TTTCATACCGCCACTGCCAACTC3′ (reverse); ABCG2, 5′-CCGCGACAGTTTCCAATGACCT-3′ (forward), 5′-GCCGAAGAGCTGCTGAGAACTGTA-3′ (reverse); ABCB4, 5′-ACCGACTGTCTACGGTCCGAA-3′ (forward), 5′-TCCATCGGTTTCCACATCAAGG-3′ (reverse); ABCA1, 5′-GCACTGAGGAAGATGCTGAAA-3′, 5′-AGTTCCTGGAAGGTCTTGTTCAC-3′, and GAPDH, 5′-ATGGAAATCCCATCACCATCTT-3′ (forward), 5′-CGCCCCACTTGATTTTGG-3′ (reverse). SYBR Green real-time PCR was performed and analyzed using the ABI PRISM 7000 Sequence Detection System software (Applied Biosystems) with reagents from the SYBR Green PCR Kit (Applied Biosystems) according to the manufacturer's instructions. Thermal cycler conditions were 95°C for 15 min, 40 cycles of 15 sec at 95°C, and finally 1 min at 60°C. GAPDH and H_2O were used as positive and negative controls, respectively. Relative expression was calculated using the comparative CT method. Expression levels were normalized to the relative levels of GAPDH.

Immunoblot analyses

To detect TNC and ABCB5 expression, cells were washed with PBS and harvested in RIPA buffer. Samples were separated on 4–12% Bis-Tris gels, transferred to polyvinylidene difluoride membranes, and then probed with either anti-human TNC (IBL America, Minneapolis, MN), anti-human ABCB5 (Rockland Immunochemicals, Inc. Gilbertsville, PA) or anti-β-actin (Sigma). To detect the signal, HRP-conjugated secondary antibody was subsequently added, followed by ECL (GE Healthcare). The immunoblot images were analyzed with Perfection 636U Scanner (EPSON) and quantitated using Scion Image Beta 4.02 software (Scion Corp.).

Animal experiments

Animal experiments were approved by the Wistar Institute's Institutional Animal Care and Use Committee. Orthotopic tumor growth was determined by subcutaneously injecting single cells suspended in growth factor reduced Matrigel® (BD Biosciences) into the right flank of 8 NOD/SCID IL2Rγ^{null} mice (NOD.Cg-*Prkdc*^{scid} *Il2rg*^{tm1Wjl}/SzJ: The Jackson Laboratory, Bar Harbor, ME) at a concentration of 5×10^5 cells per mouse. Subcutaneous tumor growth was measured twice a week for 6 weeks. For the lung colony formation assay, 2×10^5 cells were injected into 8 NOD/SCID IL2Rγ^{null} mice via the tail vein. The experiment was terminated at week 8; the lungs were harvested and subjected to histological examination. H&E staining was done on 5-μm paraffin-embedded sections by following standard protocols. Three representative frontal sections of each lung spaced 1 mm apart were analyzed. Percentage of total area occupied by lung tumor was measured using Image-Pro Plus Phase 3 Imaging System (MediaCybernetics, Bethesda, MD) based on H&E stained sections.

Statistics

Unless otherwise stated, data reported are expressed as means ± SE of at least three independent quadruplicate experiments. Statistical significance was measured using the Student's *t*-test, where $P<0.05$ was judged to be significant.

Supplementary Material

Refer to Web version on PubMed Central for supplementary material.

Acknowledgements

This work was supported by grants from the NCI (CA25874, CA47159, CA93372, CA10815).

We thank Angela Cipolla, Sarah Telson and Kate M. Belser for technical assistance. This work was also supported by Ellen Heber-Katz, James Hayden and Frederick Keeney (The Wistar Microscopy Facility), Russell Delgiacco (The Wistar Histotechnology Facility), Jonni Moore and Hank Fletcher (University of Pennsylvania, Flow Cytometry Core Facility) and The Wistar Animal Facility.

References

Bidard FC, Pierga JY, Vincent-Salomon A, Poupon MF. A "class action" against the microenvironment: do cancer cells cooperate in metastasis? Cancer Metastasis Rev. 2007

Bornstein P, Sage EH. Matricellular proteins: extracellular modulators of cell function. Curr Opin Cell Biol. 2002; 14:608–616. [PubMed: 12231357]

Brigstock DR. The connective tissue growth factor/cysteine-rich 61/nephroblastoma overexpressed (CCN) family. Endocr Rev. 1999; 20:189–206. [PubMed: 10204117]

Chiquet-Ehrismann R, Chiquet M. Tenascins: regulation and putative functions during pathological stress. J Pathol. 2003; 200:488–499. [PubMed: 12845616]

Cohen ED, Ihida-Stansbury K, Lu MM, Panettieri RA, Jones PL, Morrisey EE. Wnt signaling regulates smooth muscle precursor development in the mouse lung via a tenascin C/PDGFR pathway. J Clin Invest. 2009; 119:2538–2549. [PubMed: 19690384]

Dick JE. Stem cell concepts renew cancer research. Blood. 2008; 112:4793–4807. [PubMed: 19064739]

Fang D, Nguyen TK, Leishear K, Finko R, Kulp AN, Hotz S, et al. A tumorigenic subpopulation with stem cell properties in melanomas. Cancer Res. 2005; 65:9328–9337. [PubMed: 16230395]

Frank NY, Margaryan A, Huang Y, Schatton T, Waaga-Gasser AM, Gasser M, et al. ABCB5-mediated doxorubicin transport and chemoresistance in human malignant melanoma. Cancer Res. 2005; 65:4320–4333. [PubMed: 15899824]

Fukunaga-Kalabis M, Martinez G, Liu ZJ, Kalabis J, Mrass P, Weninger W, et al. CCN3 controls 3D spatial localization of melanocytes in the human skin through DDR1. J Cell Biol. 2006

Garcion E, Halilagic A, Faissner A, ffrench-Constant C. Generation of an environmental niche for neural stem cell development by the extracellular matrix molecule tenascin C. Development. 2004; 131:3423–3432. [PubMed: 15226258]

Goodell MA, Brose K, Paradis G, Conner AS, Mulligan RC. Isolation and functional properties of murine hematopoietic stem cells that are replicating in vivo. J Exp Med. 1996; 183:1797–1806. [PubMed: 8666936]

Grichnik JM, Burch JA, Schulteis RD, Shan S, Liu J, Darrow TL, et al. Melanoma, a tumor based on a mutant stem cell? J Invest Dermatol. 2006; 126:142–153. [PubMed: 16417230]

Helleman J, Jansen MP, Ruigrok-Ritstier K, van Staveren IL, Look MP, Meijer-van Gelder ME, et al. Association of an extracellular matrix gene cluster with breast cancer prognosis and endocrine therapy response. Clin Cancer Res. 2008; 14:5555–5564. [PubMed: 18765548]

Herlyn M, Graeven U, Speicher D, Sela BA, Bennicelli JL, Kath R, et al. Characterization of tenascin secreted by human melanoma cells. Cancer Res. 1991; 51:4853–4858. [PubMed: 1716515]

Hsu MY, Shih DT, Meier FE, Van Belle P, Hsu JY, Elder DE, et al. Adenoviral gene transfer of beta3 integrin subunit induces conversion from radial to vertical growth phase in primary human melanoma. Am J Pathol. 1998; 153:1435–1442. [PubMed: 9811334]

Jang JH, Chung CP. Tenascin-C promotes cell survival by activation of Akt in human chondrosarcoma cell. Cancer Lett. 2005; 229:101–105. [PubMed: 16157221]

Jones PL, Crack J, Rabinovitch M. Regulation of tenascin-C, a vascular smooth muscle cell survival factor that interacts with the alpha v beta 3 integrin to promote epidermal growth factor receptor phosphorylation and growth. J Cell Biol. 1997; 139:279–293. [PubMed: 9314546]

Jonker JW, Freeman J, Bolscher E, Musters S, Alvi AJ, Titley I, et al. Contribution of the ABC transporters Bcrp1 and Mdr1a/1b to the side population phenotype in mammary gland and bone marrow of mice. Stem Cells. 2005; 23:1059–1065. [PubMed: 16002779]

Kabashima A, Higuchi H, Takaishi H, Matsuzaki Y, Suzuki S, Izumiya M, et al. Side population of pancreatic cancer cells predominates in TGF-beta-mediated epithelial to mesenchymal transition and invasion. Int J Cancer. 2009; 124:2771–2779. [PubMed: 19296540]

Katoh SY, Ueno M, Takakura N. Involvement of MDR1 function in proliferation of tumour cells. J Biochem. 2008; 143:517–524. [PubMed: 18174186]

Kloepper JE, Tiede S, Brinckmann J, Reinhardt DP, Meyer W, Faessler R, et al. Immunophenotyping of the human bulge region: the quest to define useful in situ markers for human epithelial hair follicle stem cells and their niche. Exp Dermatol. 2008; 17:592–609. [PubMed: 18558994]

Kuo MT, Liu Z, Wei Y, Lin-Lee YC, Tatebe S, Mills GB, et al. Induction of human MDR1 gene expression by 2-acetylaminofluorene is mediated by effectors of the phosphoinositide 3-kinase pathway that activate NF-kappaB signaling. Oncogene. 2002; 21:1945–1954. [PubMed: 11960367]

Marchionini DM, Collier TJ, Camargo M, McGuire S, Pitzer M, Sortwell CE. Interference with anoikis-induced cell death of dopamine neurons: implications for augmenting embryonic graft survival in a rat model of Parkinson's disease. J Comp Neurol. 2003; 464:172–179. [PubMed: 12898610]

Matsuzaki Y, Besnard V, Clark JC, Xu Y, Wert SE, Ikegami M, et al. STAT3 regulates ABCA3 expression and influences lamellar body formation in alveolar type II cells. Am J Respir Cell Mol Biol. 2008; 38:551–558. [PubMed: 18096869]

Mouthon MA, Fouchet P, Mathieu C, Sii-Felice K, Etienne O, Lages CS, et al. Neural stem cells from mouse forebrain are contained in a population distinct from the 'side population'. J Neurochem. 2006; 99:807–817. [PubMed: 16925596]

Murphy-Ullrich JE. The de-adhesive activity of matricellular proteins: is intermediate cell adhesion an adaptive state? J Clin Invest. 2001; 107:785–790. [PubMed: 11285293]

Nakanishi T, Shiozawa K, Hassel BA, Ross DD. Complex interaction of BCRP/ABCG2 and imatinib in BCR-ABL-expressing cells: BCRP-mediated resistance to imatinib is attenuated by imatinib-induced reduction of BCRP expression. Blood. 2006; 108:678–684. [PubMed: 16543472]

Nilsson SK, Johnston HM, Whitty GA, Williams B, Webb RJ, Denhardt DT, et al. Osteopontin, a key component of the hematopoietic stem cell niche and regulator of primitive hematopoietic progenitor cells. Blood. 2005; 106:1232–1239. [PubMed: 15845900]

Nishii T, Yashiro M, Shinto O, Sawada T, Ohira M, Hirakawa K. Cancer stem cell-like SP cells have a high adhesion ability to the peritoneum in gastric carcinoma. Cancer Sci. 2009; 100:1397–1402. [PubMed: 19493275]

Orend G, Chiquet-Ehrismann R. Tenascin-C induced signaling in cancer. Cancer Lett. 2006; 244:143–163. [PubMed: 16632194]

Perbal B. CCN proteins: multifunctional signalling regulators. Lancet. 2004; 363:62–64. [PubMed: 14723997]

Qin XF, An DS, Chen IS, Baltimore D. Inhibiting HIV-1 infection in human T cells by lentiviral-mediated delivery of small interfering RNA against CCR5. Proc Natl Acad Sci U S A. 2003; 100:183–188. [PubMed: 12518064]

Quintana E, Shackleton M, Sabel MS, Fullen DR, Johnson TM, Morrison SJ. Efficient tumour formation by single human melanoma cells. Nature. 2008; 456:593–598. [PubMed: 19052619]

Refaeli Y, Bhoumik A, Roop DR, Ronai ZA. Melanoma-initiating cells: a compass needed. EMBO Rep. 2009; 10:965–972. [PubMed: 19680286]

Reya T, Morrison SJ, Clarke MF, Weissman IL. Stem cells, cancer, and cancer stem cells. Nature. 2001; 414:105–111. [PubMed: 11689955]

Roesch A, Fukunaga-Kalabis M, Schmidt EC, Zabierowski SE, Brafford PA, Vultur A, et al. A temporarily distinct subpopulation of slow-cycling melanoma cells is required for continuous tumor growth. Cell. 141:583–594. [PubMed: 20478252]

Scharenberg CW, Harkey MA, Torok-Storb B. The ABCG2 transporter is an efficient Hoechst 33342 efflux pump and is preferentially expressed by immature human hematopoietic progenitors. Blood. 2002; 99:507–512. [PubMed: 11781231]

Schatton T, Murphy GF, Frank NY, Yamaura K, Waaga-Gasser AM, Gasser M, et al. Identification of cells initiating human melanomas. Nature. 2008; 451:345–349. [PubMed: 18202660]

Sethi T, Rintoul RC, Moore SM, MacKinnon AC, Salter D, Choo C, et al. Extracellular matrix proteins protect small cell lung cancer cells against apoptosis: a mechanism for small cell lung cancer growth and drug resistance in vivo. Nat Med. 1999; 5:662–668. [PubMed: 10371505]

Susanto J, Lin YH, Chen YN, Shen CR, Yan YT, Tsai ST, et al. Porphyrin homeostasis maintained by ABCG2 regulates self-renewal of embryonic stem cells. PLoS One. 2008; 3:e4023. [PubMed: 19107196]

Thomson JA, Itskovitz-Eldor J, Shapiro SS, Waknitz MA, Swiergiel JJ, Marshall VS, et al. Embryonic stem cell lines derived from human blastocysts. Science. 1998; 282:1145–1147. [PubMed: 9804556]

Tuominen H, Kallioinen M. Increased tenascin expression in melanocytic tumors. J Cutan Pathol. 1994; 21:424–429. [PubMed: 7532653]

Villuendas R, Steegmann JL, Pollan M, Tracey L, Granda A, Fernandez-Ruiz E, et al. Identification of genes involved in imatinib resistance in CML: a gene-expression profiling approach. Leukemia. 2006; 20:1047–1054. [PubMed: 16598311]

Wicha MS, Liu S, Dontu G. Cancer stem cells: an old idea--a paradigm shift. Cancer Res. 2006; 66:1883–1890. discussion 1895-1886. [PubMed: 16488983]

Xu C, Inokuma MS, Denham J, Golds K, Kundu P, Gold JD, et al. Feeder-free growth of undifferentiated human embryonic stem cells. Nat Biotechnol. 2001; 19:971–974. [PubMed: 11581665]

Zhang H, Bajraszewski N, Wu E, Wang H, Moseman AP, Dabora SL, et al. PDGFRs are critical for PI3K/Akt activation and negatively regulated by mTOR. J Clin Invest. 2007; 117:730–738. [PubMed: 17290308]

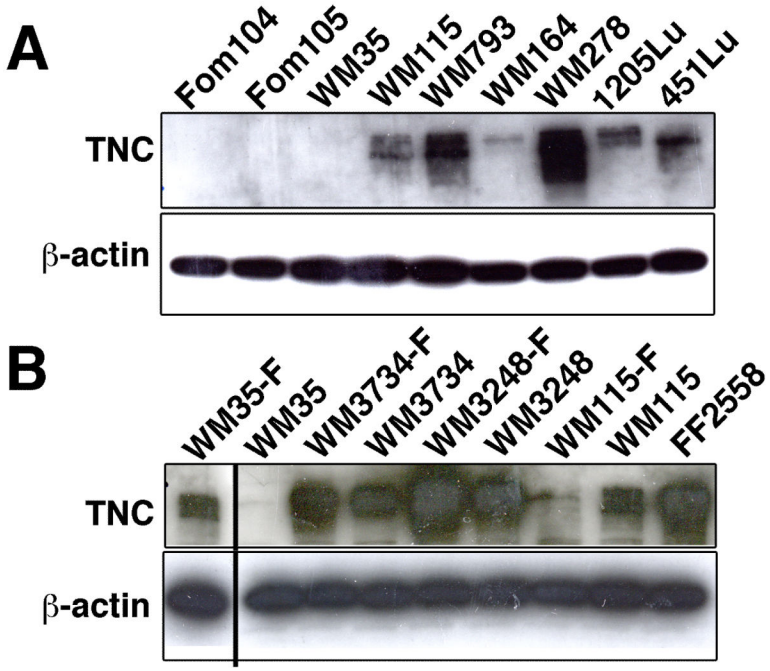

Figure 1. TNC expression is up-regulated in melanoma cells

(**A**) Immunoblot analysis to assess levels of TNC in human melanocytes and in melanoma cell lines. Increased levels of TNC in multiple melanoma cell lines as compared to normal melanocytes. Foreskin melanocytes: Fom 104 and Fom 105; melanoma cell lines: WM35, WM115, WM793, WM164, WM278, 1205Lu, and 451Lu. (**B**) TNC expression in either sphere-forming melanoma cells or adherent melanoma cells. Increased levels of TNC in sphere-forming melanoma cells (denoted with a –F suffix) as compared to adherent melanoma cells. Melanoma cell lines: WM35, WM3734, WM3248 and WM115; fibroblasts: FF2558. β-actin immunoblotting was performed as a loading control. The furthermost left lane was originally the last lane; the location was switched for clearer comparison of WM35-F and WM35.

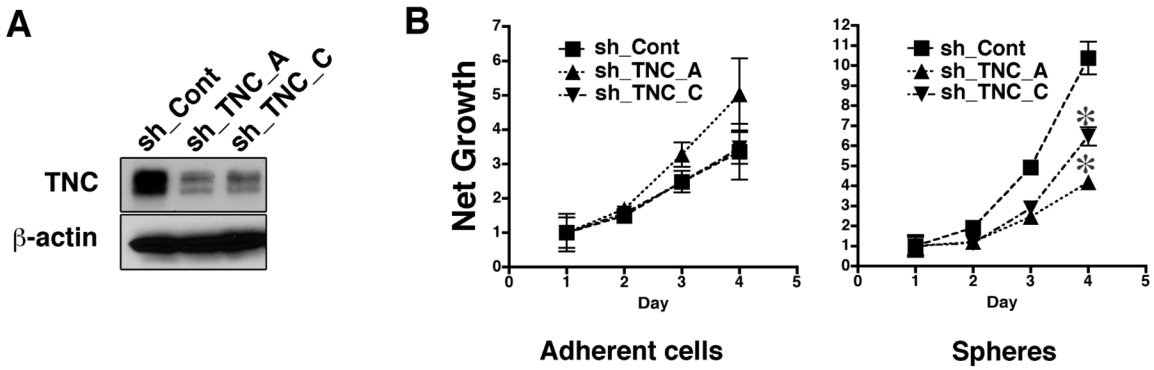

Figure 2. TNC knockdown decreases growth of melanoma spheres

(**A**) Immunoblot of WM3734 cells infected with TNC lentiviral shRNAs to two target sequences (sh_TNC_A and sh_TNC_C). A non-targeted shRNA (sh_Cont) was used as control. β-actin indicated equal loading. (**B**) Growth of WM3734 cells transduced with TNC shRNA as adherent cultures (left) and as spheres (right) was measured by MTS assay. OD 490 of each time point was normalized to Day 1. Data represent the mean ± SD (n=4). *, $p<0.05$ when compared to sh_Cont cells.

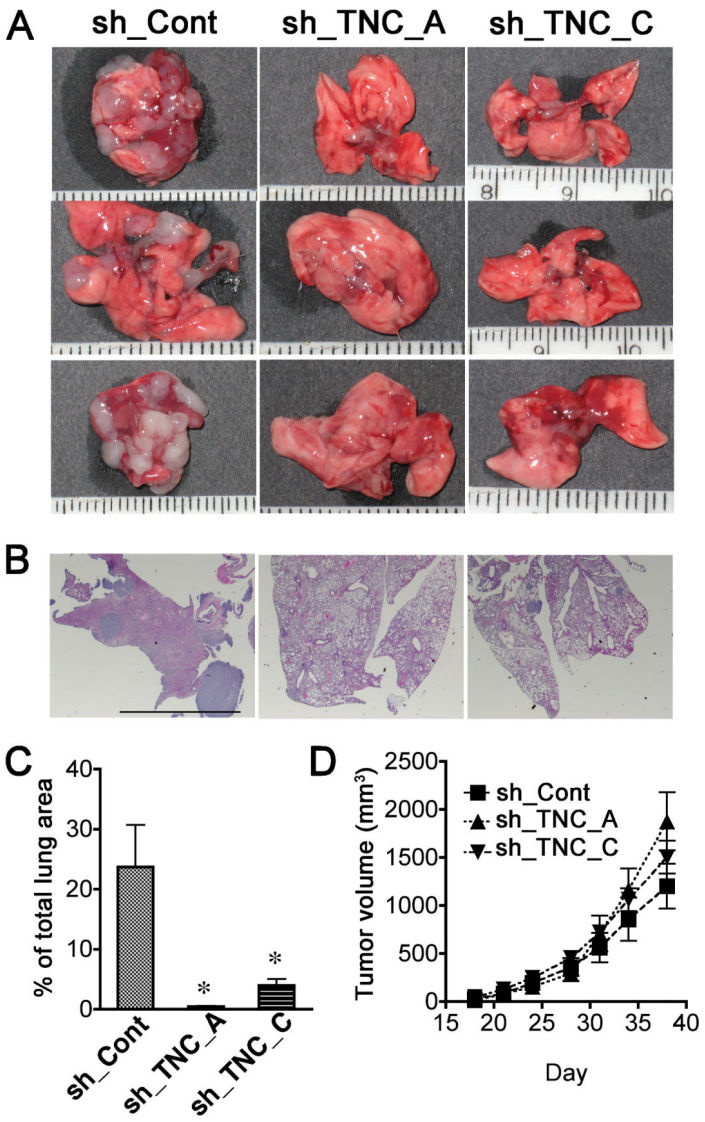

Figure 3. TNC knockdown inhibits pulmonary metastasis of melanoma cells

(A) Representative lungs showing decreased metastasis in mice injected with TNC-shRNA-expressing (sh_TNC_A or sh_TNC_C) versus control (sh_Cont) cells. 2×10^5 WM3734 melanoma cells were injected intravenously into NOD/SCID IL2Rγ^{null} mice. Mice were sacrificed after 8 weeks and the lungs harvested. (**B**) Representative lungs stained with H&E. Scale bar = 5 mm (**C**) The percentage of total area occupied by lung tumor metastases was measured based on H&E stained sections. Data are means ± SE (n=8). *$p< 0.05$, Student's *t* test. (D) WM3734 melanoma cells at a concentration of 5×10^5 cells/ mouse in 0.1mL Matrigel® were subcutaneously injected into NOD/SCID IL2Rγ^{null} mice (n=8). Mice were monitored and the tumor size was measured twice per week.

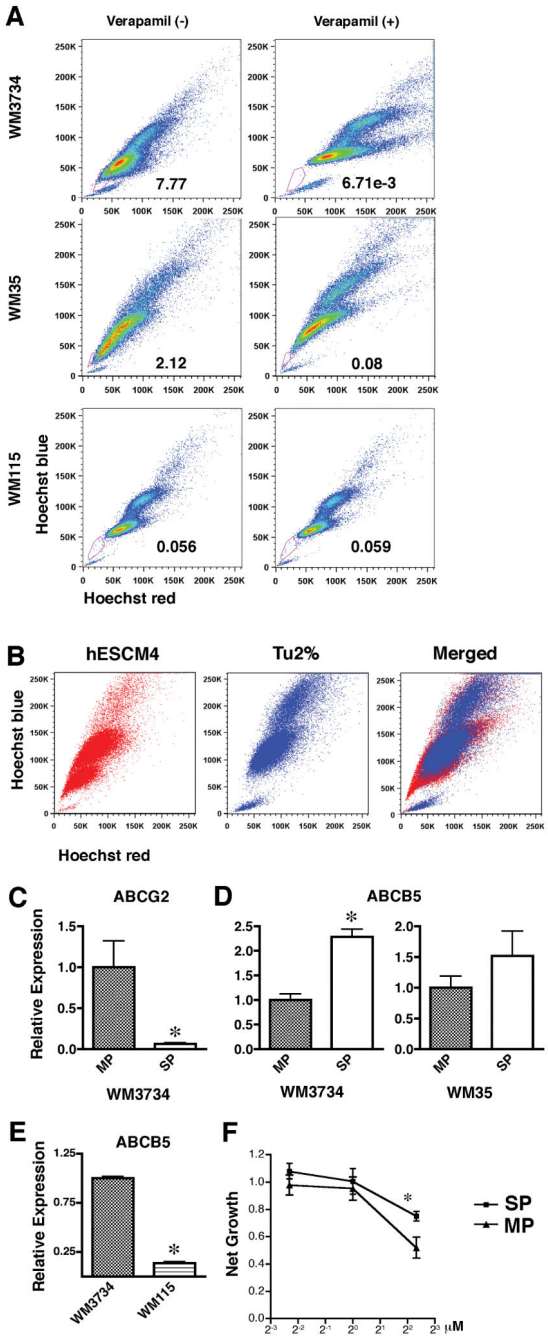

Figure 4. Melanoma spheres contain a side population fraction which expresses ABCB5 and is highly resistant to doxorubicin

(**A**) WM35, WM3734, and WM115 sphere-forming cells were stained with Hoechst 33342 dye and propidium iodide in the presence or absence of verapamil and analyzed by flow cytometry. After excluding propidium iodide-positive cells (dead cells), Hoechst dye stained cells were detected by a UV laser. When dye fluorescence was triggered at red and blue emission wavelengths, a gradient of Hoechst intensity was seen as a comma-like region on the bottom-left portion of the X-Y plot. The tip of the comma-like region included cells that

efficiently excluded the Hoechst dye, therefore showing less intensity. Incubating cells with verapamil from the beginning of the Hoechst dye exposure blocked transporters that efflux the dye, and the cells expressing verapamil-sensitive transporters became Hoechst dye-positive. The lines were drawn to gate the “side population (denoted as SP)” with verapamil-sensitive transporters, which formed the tip of the comma-like region in the absence of verapamil and disappeared in the presence of verapamil. The numbers in the plots indicate percentage of side population gate among live cells. (**B**) Hoechst dye exclusion assay revealed that WM3734 melanoma sphere cells contained a larger SP fraction than WM3734 adherent cells. (**C**-**D**) WM3734 spheres sorted by flow cytometry for SP and major population (MP) cells. (**C**) qRT-PCR shows higher expression levels of ABCG2 in WM3734 MP cells compared to the SP. Data were normalized to GAPDH. The data are presented as means ± SE. (n=4) $p<0.05$ when compared to MP cells. (**D**) qRT-PCR shows higher expression levels of ABCB5 in WM3734 SP cells compared to the MP. Data were normalized to GAPDH. Data are expressed as means ± SE. (n=4) $p<0.05$ when compared to MP cells. (**E**) qRT-PCR shows higher expression levels of ABCB5 in WM3734 cells compared to WM115 cells. Data were normalized to GAPDH. Data are expressed as means ± SE. (n=4) *, $p<0.05$ when compared to WM3734 cells. (**F**) Dose response curves showing a shift in the SP compared to the MP, suggesting SP cells are more resistant to doxorubicin. Following cell sorting SP and MP cells, in single cell suspension, were plated in 96-well plates at a concentration of 10,000 cells/well in hESCM4 medium. 24 hours later, various concentrations of doxorubicin were added. The MTS assays were performed 72 hours post drug treatment. The data were normalized to the doxorubicin-untreated control. *, $p<0.05$ when compared to MP cells.

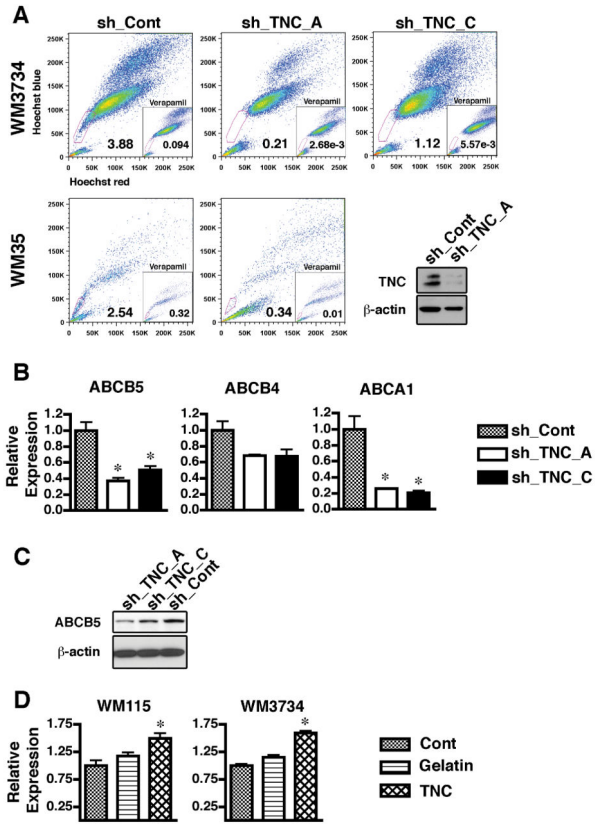

Figure 5. TNC knockdown decreases SP fraction in melanoma sphere cells

(**A**) Hoechst dye exclusion assay showed that the percentage of SP cells was dramatically decreased in TNC lentiviral shRNA infected WM3734 (upper panels) and WM35 cells (lower panels). Lower right panel – immunoblot showing efficacy of TNC knockdown (sh_TNC_A) in WM35 cells compared to non-targeting shRNA (sh_Cont). β-actin indicates equal loading. **(B)** Gene expression of ABCB5, ABCB4 and ABCA1 was down-regulated in TNC lentiviral shRNA transfected cells. qRT-PCR analysis was performed using transporter-specific primers. Data were normalized to GAPDH and expressed as means ± SE. (n=4) $p<0.05$ when compared to sh_Cont cells. (**C**) Immunoblot showing that protein expression of ABCB5 is decreased in WM3734 cells transduced with TNC shRNA (sh_TNC_A and sh_TNC_C) when compared to non-targeting shRNA (sh_Cont). β-actin indicates equal loading. (D) Gene expression of ABCB5 was up-regulated in WM115 melanoma spheres (left) and WM3734 adherent cells (right) treated with 10 μg/ml human TNC for 24 hours. Cont: control cells cultured in regular medium. Gelatin: cells cultured in presence of 10 μg/ml gelatin matrix. qRT-PCR analysis was performed using ABCB5-specific primers. Data were normalized to GAPDH and expressed as means ± SE. (n=4) $p<0.05$ when compared to Cont cells.

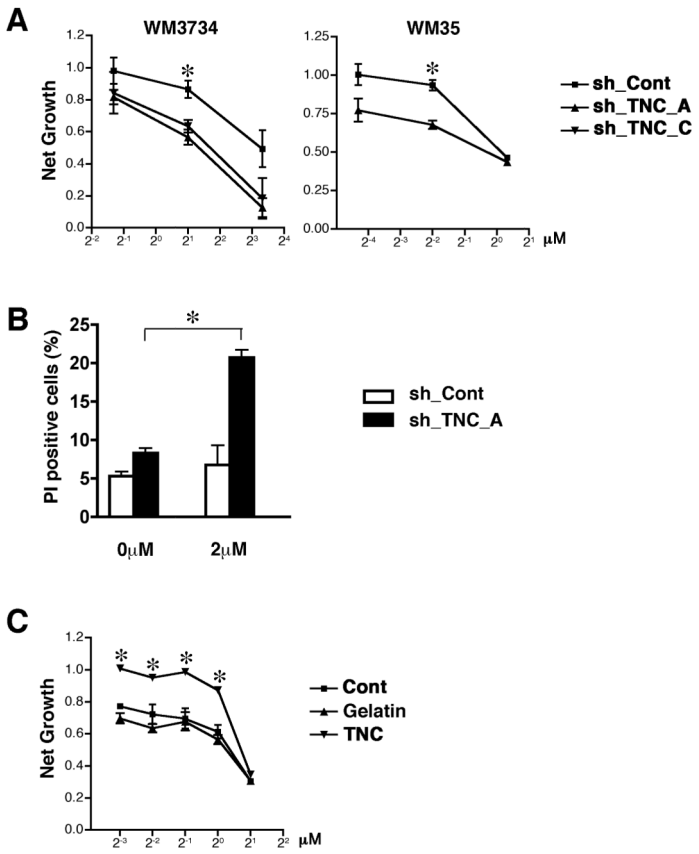

Figure 6. TNC knockdown potentiates doxorubicin response

(**A**) Depletion of TNC with shRNA sensitizes melanoma cells to doxorubicin treatment, demonstrated as a shift of the sh_TNC dose response curves compared to sh_Cont cells. sh_TNC and sh_Cont cells were dissociated into single cell-suspensions in hESCM4 medium, which was conditioned for 7 days with each lentiviral infected cell line, and plated in 96-well plates at a concentration of 10,000 cells/well. Twenty-four hours later, various concentrations of doxorubicin were added. The MTS assays were performed 72 hours post drug treatment. The data were normalized to the doxorubicin-untreated control. *, $p<0.05$ when compared to sh_Cont cells. (**B**) Apoptosis assessed by propidium iodide (PI) staining of untreated and 2μM doxorubicin-treated WM3734 sh_Cont cells and sh_TNC_A cells 24 hours post-treatment. Columns indicate propidium iodide-positive apoptotic cells. Twenty-four hour treatment with 2μM doxorubicin induced apoptosis in sh_TNC_A cells but did not impair survival of sh_Cont cells. ($n = 3$) *, $p<0.05$ when compared to untreated cells. (**C**) Exogenous TNC increases doxorubicin resistance, demonstrated as a shift in the dose response curves. WM115 sphere cells were dissociated into single cell-suspensions in hES medium and plated in 96-well plates at a concentration of 10,000 cells/well. Cont: without additional reagent. Gelatin: with 10 μg/ml gelatin matrix. TNC: with 10 μg/ml human TNC. Twenty-four hours later, various concentrations of doxorubicin were added. The MTS assays were performed 72 hours post drug treatment. The data were normalized to the doxorubicin-untreated control. *, $p<0.05$ when compared to Cont cells.